A Novel Self-Aligned Fabrication Process for Nickel-Indiffused Lithium Niobate Ridge Optical Waveguides

Wen-Ching Chang, Chao-Yung Sue, Hung-Ching Hou, Shih-Jung Chang, and Pei-Kuen Wei

***Abstract*— A novel self-aligned fabrication process for Ni : $LiNbO_3$ ridge waveguides has been proposed. By using the self-aligned trilayered structure composed of Ni/Ti/Si, the fabrication process is significantly simplified, and takes advantage of suppression of the unwanted planar waveguides and high-coupling efficiency to a single-mode fiber as compared to the conventional processes. Detailed investigations into the characteristics of the ridge waveguides have also proved to be informative under different fabrication parameters. Moreover, the novel self-aligned fabrication process was applied to fabricate a ridge waveguide Mach–Zehnder modulator. The measured half-wave voltage and extinction ratio were 20.5 V and 12 dB (@ 1.3 μm), and were 4.2 V and 8 dB (@0.6328 £gm).**

***Index Terms*— Diffusion, electrooptic, etch, integrated optics, modulator, optical field, waveguide.**

I. Introduction

In recent years, broad-band optical communication systems has attracted much research and stimulated great development in high-speed integrated optics devices. The key problem of wide-band modulators is the limitation in the bandwidth that arises from the high dielectric constant of lithium niobate ($LiNbO_3$) itself, which leads to velocity-mismatch between the modulated microwave signal and optical field. Hence, the best way to reduce the effective microwave index is to replace $LiNbO_3$ crystal with low dielectric constant materials, such as silicon oxide (SiO_2) or the air around traveling-wave electrodes [1]. To achieve better frequency responses, several velocity-matching structures, such as thick electrodes [2], [3], shielding ground plane [4], [5], and ridge waveguides [6], [7], have been proposed. Noguchi *et al.* proposed a broadband Mach–Zehnder modulator with a ridge structure and thick electrodes [7]. The structure enhances the overlap integral between microwaves and optical fields under the conditions of velocity matching and impedance matching.

Due to the strong etch resistance of $LiNbO_3$, dry etch methods, such as plasma etching [8] and reactive ion etching [9], were the traditional techniques for the fabrication of ridge waveguides. Though the etch rate has been speeded up through the introduction of structural defects by the physical bombardment, the etched surfaces of the ridge structure were excessively rough, rendering them unsuitable for practical applications. In 1992, Laurell *et al.* proposed a new wet etch technique for proton-exchanged (PE) $LiNbO_3$ [10]. It has been demonstrated that the PE regions on the c^+-face can be etched away by the mixture of hydrofluoric acid (HF) and nitric acid (HNO_3), while the regions without proton-exchanging are left essentially untouched. Following the PE wet etch technique, much research that focused on the fabrication of ridge waveguide Mach–Zehnder modulators have been completed [11]–[13] successfully. Lee *et al.* first fabricated a ridge waveguide Mach–Zehnder modulator in x-cut $LiNbO_3$ [11]. Cheng *et al.* demonstrated ridge waveguide Mach–Zehnder modulators by the PE wet etching technique in both z-cut and y-cut $LiNbO_3$ [12], [13]. To our knowledge, PE process produced serious surface damages in y-cut $LiNbO_3$. While the interaction depth in the PE region exceeds a critical value of 2 μm [14], a large stress caused by the PE process must be released through the formation of crystal cracks along the x-axis in y-cut $LiNbO_3$. Thus, some protective techniques, such as the nickel indiffusion proton exchange (NIPE) and the buffered PE melt [13] techniques should be applied to slow down the PE rate, which makes the PE wet etch of y-cut substrate possible.

In [15], Chen *et al.* proposed two fabrication processes for ridge waveguides, which were nickel (Ni) diffusion prior to PE wet etch, the DE process, and PE wet etch prior to Ni diffusion, the ED process. Though these processes have been optimized and are much better than the conventional dry etch methods, further improvement is necessnary. This is because the former easily results in unwanted planar waveguides flanking the ridge structures, while the latter requires relatively complicated process. In this paper, a novel self-aligned processing technique for the fabrication of $LiNbO_3$ ridge waveguides was proposed. As the Ni diffusant, titanium (Ti) diffusion barrier, and silicon (Si) PE mask are exactly self-aligned on the waveguide regions, the fabrication process is significantly simplified as compared to the traditional process of ridge waveguides. In addition, detailed analysis into the characteristics of ridge waveguides, such as etch rate, etch depth, surface roughness and surface profile, have been sucessfully investigated by varying the diffusion parameters and the PE

Manuscript received July 9, 1998; revised December 4, 1998. This work was supported by the National Science Council, Taipei, Taiwan, Republic of China under Contract NSC 87-2215-E-032-001. The work was done in Integrated Optics Laboratory, National Taiwan University, R.O.C.

W.-C. Chang is with the Department of Electrical Engineering, Tamkang University, Tamsui, Taipei Hsien, Taiwan 25137 R.O.C.

S.-J. Chang is with the Department of Electrical Engineering, National Taiwan University, Taipei 10617, Taiwan, R.O.C.

P.-K. Wei is with the Institute of Atomic and Molecular Sciences, Academia Sinica, Taipei 10617 Taiwan, R.O.C.

Publisher Item Identifier S 0733-8724(99)02687-0.

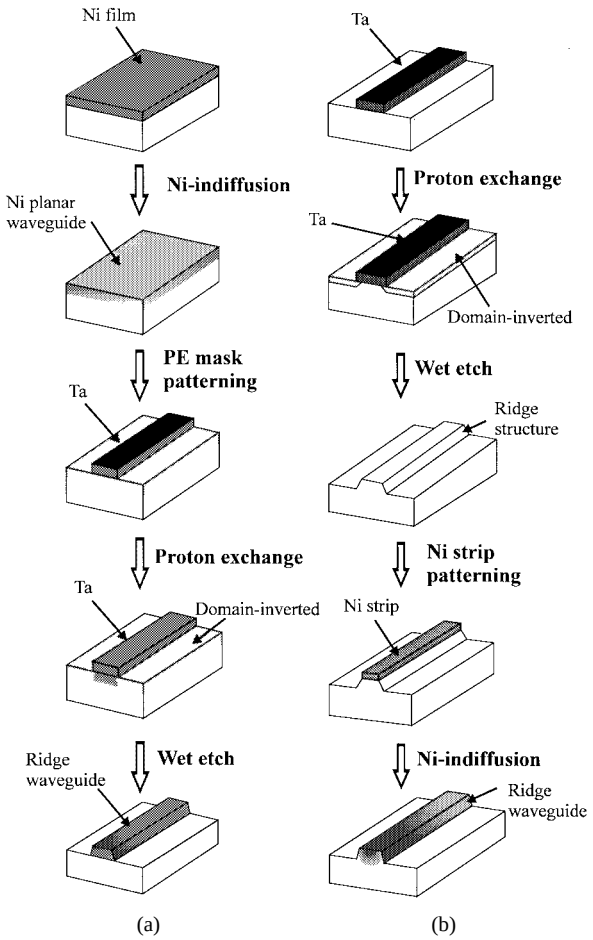

Fig. 1. Traditional fabrication process for $Ni:LiNbO_3$ ridge waveguides [15]: (a) Ni diffusion prior to PE wet etch (the DE process) and (b) PE wet etch prior to Ni diffusion (the ED process).

conditions. Moreover, the electrooptical (EO) characteristics of the ridge waveguides fabricated by the self-aligned process were examined through the fabrication and measurement of a ridge waveguide Mach–Zehnder modulator. The measured half-wave voltage and the extinction ratio are 20.5 V and 12 dB at a wavelength of 1.3 μm, and are 4.2 V and 8 dB at a wavelength of 0.6328 μm.

This paper is organized as follows. Section II describes the comparison between the traditional process and the proposed self-aligned process of the $Ni:LiNbO_3$ ridge waveguides. Section III shows effects of fabrication conditions on the characteristics of ridge waveguides fabricated by the self-aligned process. Finally, Section IV is the conclusion.

II. Novel Self-Aligned Process for Ridge Waveguides

A. Traditional Fabrication Process

According to [15], the fabrication process for ridge waveguides can be catagorized into two kinds: the DE process and the ED process. The former technique was illustrated in Fig. 1(a), while the latter technique in Fig. 1(b).

The DE process is shown in Fig. 1(a), a layer of Ni film is first deposited on the c^+-face by a thermal evaporator, and then diffused at high temperature (800–950 °C) to form a planar waveguide. To make a ridge structure, the planar waveguides are covered with a patterned PE mask of tantalum (Ta), and followed by the PE wet-etching technique. However, the previously indiffused Ni planar waveguides will inhibit the proton-exchanged effect, which is the so-called NIPE effect [13], [16]. As a result, the PE depth usually does not exceed the diffusion depth of Ni planar waveguides. In other words, the residues of the wet etching on the PE regions will become unwanted planar waveguides, which will seriously interfere the guiding ability of the ridge waveguides. Though the unwanted planar waveguides will be separated from the ridge waveguides by using the postannealing technique after the PE process. Unfortunately, however, unstable results have made an unpronounced improvement.

The ED process shown in Fig. 1(b) is the alternative fabrication technique for ridge waveguides. At first, a PE mask of Ta is patterned on the c^+-face of $LiNbO_3$. Using the PE wet etching technique, bulk $LiNbO_3$ is etched to form a ridge structure with fairly smooth etched surfaces [15]. To enhance the optical confinement in the vertical direction, Ni strips are patterned on the top of the ridge structure by the lift-off process, and then diffused in an oven to form a ridge waveguide. Most importantly, mask alignment in the second photolithographic process becomes the critical step for better optical guiding performance. That is to say, either a better mask-aligned equipment or an accurate mask-aligned technique is necessary to maintain satisfying yields. Hence, we proposed an alternative fabrication technique, the self-aligned process, for further amelioration. By using this technique, it requires only one photolithographic process, such that the fabrication process is significantly simplified. Moreover, this process has the additional advantage of suppression of the unwanted planar waveguides compared to the DE process.

B. Novel Self-Aligned Process

1) Fabrication Process: The fabrication process for the self-aligned technique is illustrated in Fig. 2. At first, the patterns of waveguides are transferred onto the $LiNbO_3$ substrate by the photolithographic process. Then, the diffusant of Ni, the diffusion barrier of Ti, and the PE masks of Si are successively deposited on the substrate by an E-beam evaporation system. By immersing the samples in acetone (ACE), which is the lift-off process, the trilayered structure composed of Ni/Ti/Si is left on the substrate with good adhesion and exact alignment. Putting the sample into the oven, diffusion process is performed under 800–900 °C for several hours to drive Ni atoms into the $LiNbO_3$ substrate. As the required indiffusion temperature for Ti film is always higher than 1000 °C, Ti/Si will be left on the substrate after Ni-indiffusion. This is because the diffusion coefficient of Ti is smaller than that of Ni, therefore Ti layer functions as a diffusion barrier.

Interestingly, the samples are preheated at 400 °C for 1 h to make the Si PE mask more condensed and have better adhesion between each layers during the diffusion process. With the protection of the PE mask formed by the combination of Ti and

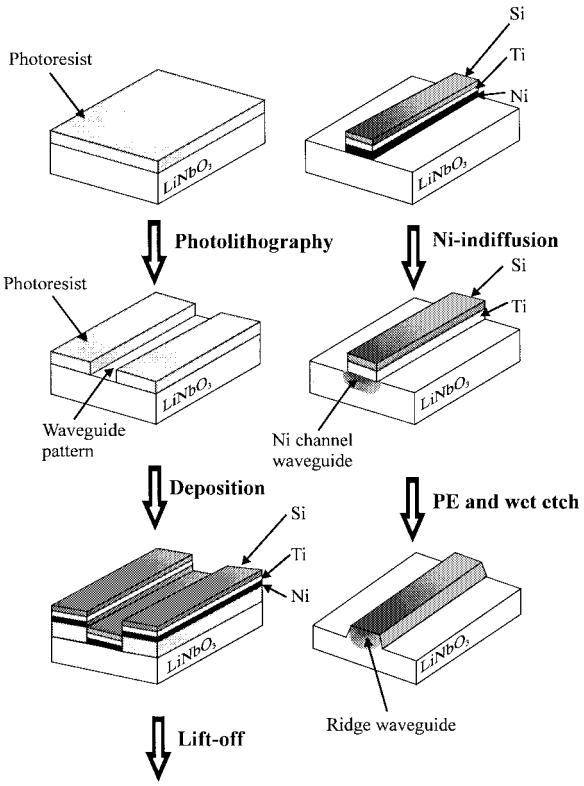

Fig. 2. The novel self-aligned fabrication process for $Ni:LiNbO_3$ ridge waveguides.

Si, the regions not protected by the PE mask will be domain-inverted in the molten benzoic acid, and then will be etched in pure HF, completing the fabrication of a $Ni:LiNbO_3$ ridge waveguide. In our proposed processs, pure HF is used as the etch solution instead of the mixture of HF and HNO3 [10]. According to our observations, HF also results in smooth and uniform etched surfaces. For this reason, HF is an alternative choice for the wet etching of proton-exchanged $LiNbO_3$.

2) Trilayered Structure: In this work, the waveguides are formed by Ni indiffusion to give its superior properties of process-dependent polarization and relatively low diffusion temperature [17], [18]. On the other hand, the diffusion barrier should have the following properties: slower diffusion rate (requiring a higher diffusion temperature in comparison with Ni), strong etch resistance to benzoic acid, and good adhesion to Ni film. Among the materials of interests, Ti, ZrO_2, and Ta are under considerations for the diffusion barrier. However, ZrO_2 is not easily etched away in HF, while Ta film is prone to getting worse after heat-treatment. Thus, Ti become the best choice for the diffusion barrier.

In consideration of the PE mask, Ta, Si, and Au have better etch resistence to benzoic acid than do other materials. Because Ta is not suitable for heat-treatment and Au is poor for adhension, Si is the best choice. Based on our observations, the deposited thickness of the self-aligned structure (Ni/Ti/Si) will determine the qualities of the ridge waveguides. It has been proved that Ni diffusant of 300 Å (for a waveguide with extraordinarily polarization at a wavelength of 1.3 μm), Ti diffusion barrier of 700 Å, and Si PE mask of 3000 Å become the best combination for the self-aligned process.

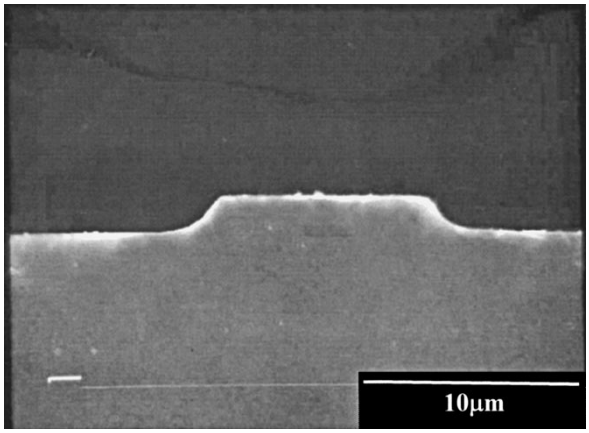

(a)

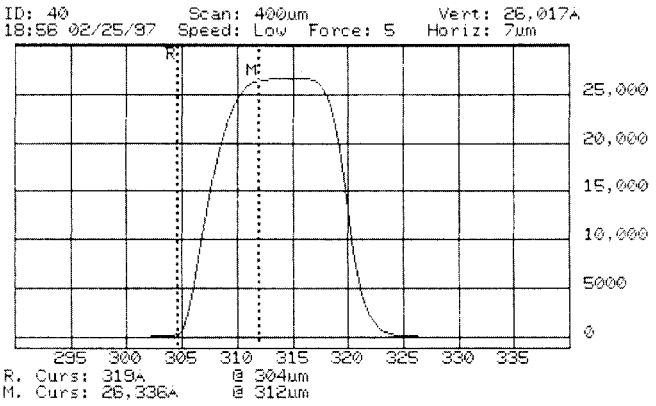

(b)

Fig. 3. Cross-sectional view of the ridge waveguide by using the self-aligned process (diffused at 850 °C for 2.25 h, PE at 240 °C for 6 h): (a) SEM photograph and (b) surface profile.

3) Determination of Proton Source: The PE process involves a chemical reaction between the lithium ions (Li^+) which outdiffuse from the $LiNbO_3$ substrate and the protons (H^+) which come from the proton source. In general, the most commonly used poton sources are benzoic acid and pyrophosphoric acid. Because pyrophosphoric acid has a relatively stronger acidity than does benzoic acid, small tiny pits on the ridge waveguides can not be prevented despite of using the Ta mask. Hence, benzoic acid is the most suitable proton source for our self-aligned process. In contrast, pits seldom appear on the ridge structure after the combination of Ti/Si is preheated to enhance its etch resistance.

4) Measurement of the Ridge Waveguides: The efficiency of the self-aligned process is demonstrated by measuring the characteristics of the ridge waveguides. The samples are deposited with the self-aligned structures composed of Ni/Ti/Si (300 Å/700 Å/3000 Å) as previously discussed. After being preheated at 400 °C for 1 h, the samples with the self-aligned structure are diffused at 850 °C for 2.25 h and 900 °C for 1 h. The PE process is performed at 240 °C for different times, and then wet etched in HF for 6 h. Fig. 3(a) shows the cross-sectional SEM photograph of the ridge waveguide fabricated by the self-aligned process, which is diffused at 850 °C for 2.25 h and proton exchanged at 240 °C for 6 h. Fig. 3(b)

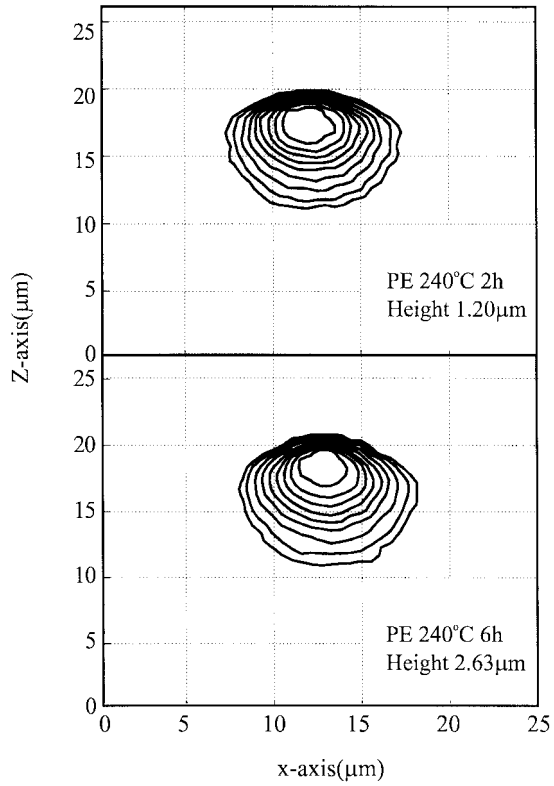

Fig. 4. Optical contour profiles of the fundamental TM mode of the ridge waveguide fabricated by the self-aligned process at a wavelength of 1.3 μm. (Diffused at 900 °C for 1 h, PE at 240 °C for 2 and 6 h.)

shows the surface profile of the ridge waveguides fabricated by the same process and condition. The original width of the mask opening is 12 μm. From Fig. 3(a) and (b), the ridge waveguide has a etched depth of 2.60 μm, a lateral etched width of 1.46 μm, and a calculated tilt angle of 61°.

Alternatively in another experiment, the samples which are diffused at 900 °C for 1 h are divided into three sets, followed by proton exchange at 240 °C for 2, 4, and 6 h. After the wet etch process, all samples are measured by a surface stylus profiler. The measured etch depths are 1.20, 2.06, and 2.63 μm. To observe the optical confinement of the ridge waveguides, all samples are end-polished for the convenience of end-fire coupling. The waveguides are all measured by a CCD camera at the wavelength of 1.3 μm. Fig. 4(a) and (b) shows the optical contour profiles of the fundemental TM mode of the ridge waveguides fabricated under the PE conditions of 240 °C for 2 and 6 h. The optical-field patterns and their spot sizes of these waveguides are measured. The spot size at $1/e$ intensity is 8.5 μm in width and 7.5 μm in depth for the waveguide under the PE time of 2 h, and is 8 μm in width and 7.8 μm in depth for the waveguide under the PE time of 6 h.

On the other side, the coupling efficiency between optical waveguides and a single-mode fiber is a function of index differences and the overlap integral. The overlap integral between the optical field of the 1.3-μm ridge waveguide and that of a single-mode fiber is 96% for the waveguide under the PE time of 2 h, and is 94% for the waveguide under the PE time of 6 h. It has been summarized that the field pattern of the ridge waveguide fabricated by the self-aligned process

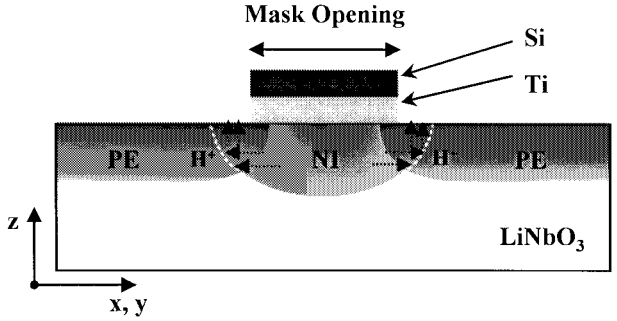

Fig. 5. Mechanism of the NIPE effect (schematically represented by the dashed arrow) on the self-aligned process.

is fairly close to that of the single-mode fiber, and thus it takes the advantage of high-coupling efficiency as compared to the conventional $LiNbO_3$ optical waveguides, such as Ti-indiffused and proton exchanged techniques.

Finally, it was found that the propagation loss of the waveguide fabricated by the self-aligned process was larger than that of Ti-indiffused $LiNbO_3$ waveguide. This is because the surface of the ridge waveguide is not as smooth as that fabricated by the Ti-indiffusion techniques. Accordingly, the rough surface of the ridge waveguide would result in the scattering loss. Its mechanism and the method of improvement will be described in Section III-C.

III. Characteristics of Ridge Waveguides By Self-Aligned Process

According to the reports cited, Ni has the so-called NIPE effect of inhibiting proton H^+ to exchange with Li^+ ions [13], [16]. Moreover, the effect is more pronounced under higher Ni concentration [16]. Once the NIPE effect occurs, the wet etching is inhibited. From our experimental results, the effect also occurs in the self-aligned process. This is because the indiffusion of Ni produces an isotropically graded concentration profile, which influences the surface profile of the ridge waveguides accordingly. The mechanism of the NIPE effect on the self-aligned process is schematically shown in Fig. 5. From this figure, it is obvious that the NIPE effect on the self-aligned process occurs in both the vertical and the lateral direction. At first, the lateral diffusion of Ni atoms will inhibit proton exchange at the edges of the PE mask. Hence, the etch depth in the vertical direction near the sidewall regions is reduced. Secondly, the NIPE effect in the lateral direction depends on the Ni concentration profile. Aa a result, lateral wet etching of the ridge structure is affected. For these reasons, the surface profile of the ridge waveguides will be influenced by the NIPE effect.

On the other hand, it is well known that Ti-indiffusion will induce domain inversion in $LiNbO_3$. In addition, the domain inversion regions will be etched by the mixture of HF and HNO_3. Accordingly, it was predicted that Ni indiffusion would also induce domain inversion in the self-aligned process. However, because the diffusion temperature of Ni is much lower than that of Ti, the effect tends to not be pronounced. To further demonstrate these predictions, a series of experiments have been completed and are described as follows.

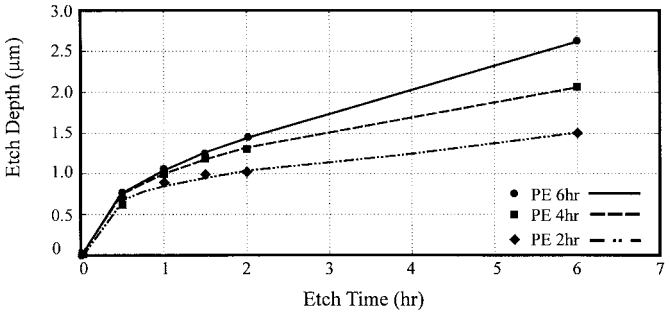

Fig. 6. Etch depth as a function of etch time under the PE conditions of 240 °C for 2, 4, and 6 h (diffused at 850 °C for 2.25 h).

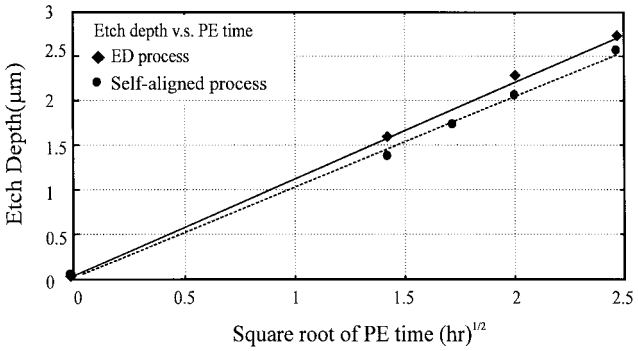

Fig. 7. Etch depth as a function of square root of the PE time for both the ED process and the [WW1] self-aligned process (self-aligned process: diffused at 900 °C 1 h, and both processes: PE at 240 °C in molten benzoic acid).

A. Etch Rate

Fig. 6 shows the etch depth as a function of the etch time under different PE conditions. The samples with the self-aligned structure are diffused at 850 °C for 2.25 h after having been preheated at 400 °C for 1 h. Then, the samples are put in sealed bakers filled with benzoic acid, and heated in the oven with temperature up to 240 °C. Then the PE process is performed at 240 °C for 2, 4, and 6 h. Then, the samples are immersed in pure HF, and are taken out every half an hour to measure their etch depth. As it is shown in Fig. 6, the waveguide has a larger etch dpeth under a longer PE time. Furthermore, the etch rate is higher during the first two hours than it is during the last four hours. In addition, Fig. 6 reveals that the etch rate is gradually saturated after 6 hs' wet etching.

B. Etch Depth

Furthermore, the etch depth for the self-aligned process is reduced compared with the ED process, as shown in Fig. 7. The solid line represents the etch depth as a function of square root of the PE time for the ED process, while the dash line represents that for the self-aligned process. For both fabrication processes, the samples are proton-exchanged at 240 °C for different times. Obviuosly, the final etch depth of the ridge waveguide is proportional to the square root of the PE time, and the etch depth of the ridge waveguides fabricated by the ED process is slightly higher than that by the self-aligned process. This is because previously indiffused Ni

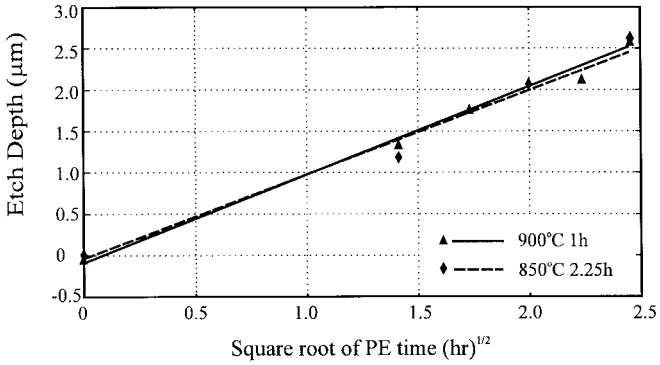

Fig. 8. Etch depth as a function of square root of PE time in z-cut $LiNbO_3$ by using the self-aligned process (PE at 240 °C in benzoic acid).

atoms slightly induce domain-inversion, which causes slight wet etching on the waveguide surface. This effect can be ameliorated by operaing at a lower diffusion temperature (such as 750–800 °C.

Fig. 8 shows the final etch depth as a function of the square root of PE time at 240 °C in z-cut $LiNbO_3$ by using the self-aligned process. The solid line represents the samples which are diffused at 850 °C for 2.25 h; while the dash line at 900 °C for 1 h. From the above two diffusion conditions, single TM mode Ni : $LiNbO_3$ ridge waveguides with good optical confinement can be obtained. Obviously, the etch depth of the ridge waveguide by the above two diffusion conditions are quite colse. In other words, the effect of Ni-indiffusion induced domain-inversion on the two waveguides is almost the same.

C. Surface Roughness

Fig. 9(a)–(d) shows the SEM photographs from the top view of the ridge waveguides fabricated under the diffusion conditions of 900 °C for 1 h, 850 °C for 1 h, 800 °C for 1 h, and 750 °C for 1 h. All samples are proton exchanged at 240 °C for 6 h, and wet etched in HF for 6 h. According to our observations, the etch surfaces of the ridge waveguides become smoother while the diffusion temperature was reduced below 800 °C. This phenomenon is caused by two reasons. The first reason is that Ni-indiffusion will slightly induce domain-inversion on the waveguide regions. Once the domain-inversion effect happens, the surface of the Ni-indiffused ridge waveguides will be etched and then leave sligntly rough surfaces. Interestingly, the domain-inversion induced by Ni-indiffusion is not pronounced under a lower diffusion temperature. The other reason is that a higher diffusion temperature will degrade the protection capability of Ti and Si films. On the contrary, a lower diffusion temperature will maintain a better etch resistance for the PE mask. For the above reasons, Ni-idiffusion at a lower temperature is suitable for the self-aligned process.

D. Surface Profile

From the above discussions, it is clear that NIPE effect in the self-aligned process influences the surface profile of the ridge waveguide. To further demonstrate this result, we utilized both the ED process and the self-aligned process to fabricate

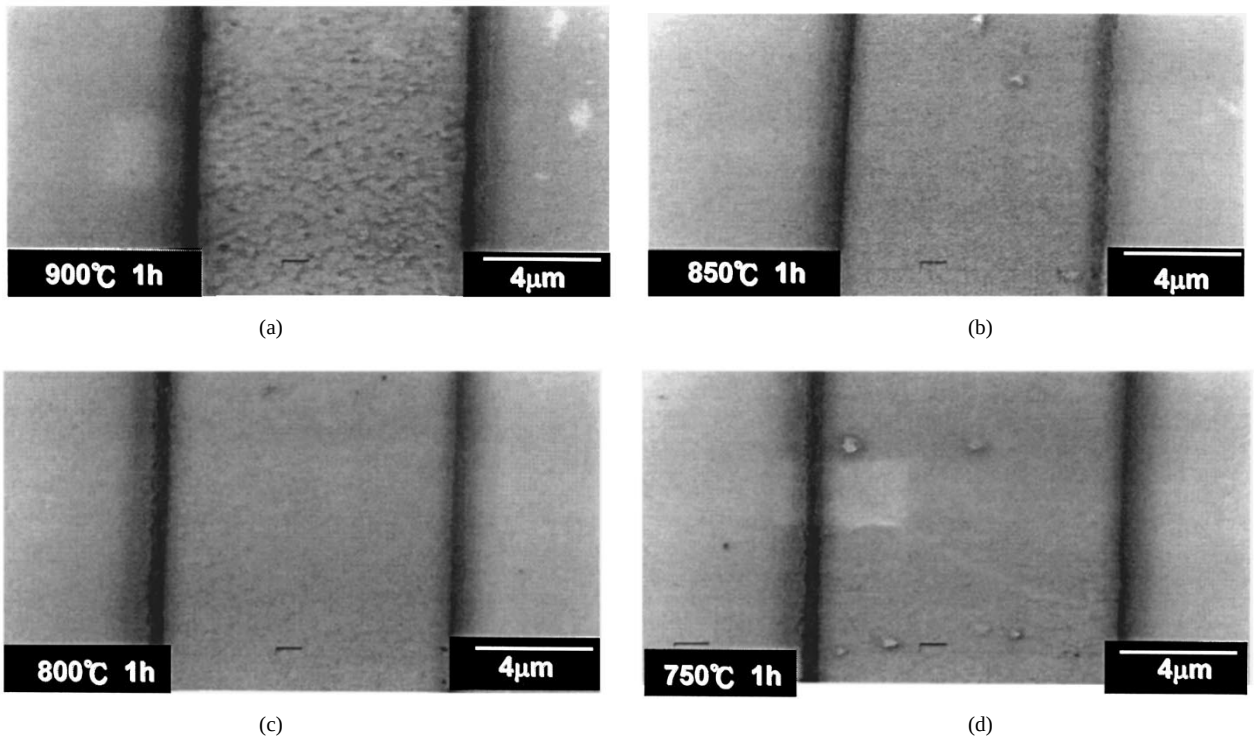

Fig. 9. SEM photographs from the top view of the ridge waveguides fabricated by the self-aligned process under different diffusion temperatures: (a) 900 °C, (b) 850 °C, (c) 800 °C, and (d) 750 °C.

the ridge waveguides. Fig. 10 shows the cross-sectional SEM photograph of the ridge waveguides. Fig. 10(a) is the SEM photograph corresponding to the ED process and Fig. 10(b) corresponds to the self-aligned process. In both cases, the PE process is performed at 240 °C for 6 h, and followed by the wet etching in HF for 6 h. Comparing Fig. 10(a) with Fig. 10(b), it is obvious that the surface profile of the ridge structure is influenced by the Ni concentration profile. In other words, the vertical NIPE effect will reduce the vertical etch depth near the sidewall regions, while the lateral NIPE effect will inhibit the lateral wet etching. For this reasons, the surface profile of the ridge waveguide is influenced by the Ni concentration profile.

E. Device Fabrication

The electrooptic effect of the Ni : $LiNbO_3$ ridge waveguides was examined through the fabrication and measurement of Mach–Zehnder modulators. The structure of the device is designed as follows: a waveguide width of 8 μm, a full branch angle of 1°, an electrode gap of 15 μm, and an electrode length of 1 cm. Utilizing photolithography, film deposition, and lift-off process, the self-aligned structure composed of Ni/Ti/Si (300 Å/700 Å/3000 Å) is patterned on the substrate with an exact alignment. The diffusion process is performed at 900 °C for 1.5 h, and the PE process is preceded in molten benzoic acid at 240 °C for 6 h, followed by the wet etch in HF for 6 h. Fig. 11 shows the SEM photograph of a ridge waveguide Mach–Zehnder modulators, where the Y-branch region of the modulator is shown. To measure the electrooptic effect, the modulator is covered with a 1500 Å-thick SiO_2 buffer layer and a 3000 Å-thick Al layer to form the electrodes in the interaction region.

Fig. 12 shows the modulation output of the Ni : $LiNbO_3$ ridge waveguide Mach–Zehnder modulator. Fig. 12(a) is measured at a 0.6328 μm wavelength, and the half-wave voltage is 4.2 V, and the extinction ratio is 8 dB. Another experiment has been measured at a wavelength of 1.3 μm, the half-wave voltage is 20.5 V and the extinction ratio is 12 dB. The lower extinction ratio of 8 dB results mainly from asymmetry of the Y-branch. The Y-branch of the modulator is inevitably asymmetric after the lithographic process acompanied with fabrication errors. According to a simple calculation, a little deviation from the waveguide symmetry in the Y-branch would dramastically decrease the extinction ratio. It could be expected that reducing the fabrication error would increase the extinction ratio.

The half-wave voltage of the modulator measured at a 1.3 μm wavelength is larger than that at 0.6328 μm. It is well-known that the half-wave voltage is mainly depedent on the overlap integral between the electrical and optical fields, the operating wavelength, and the linear EO coefficient. According to the above data at 0.6328 μm and following a simple calculation, the half-wave voltage at 1.3 μm could be estimated as nearly 10 V. Nevertheless, the mode size of the waveguide at 1.3 μm is larger than that at 0.6328 μm. Thus, the half-wave voltage is increased due to the decrease of the overlap integral.

IV. Conclusion

In this paper, a novel self-aligned fabrication process for Ni:$LiNbO_3$ ridge waveguides has been proposed. Detailed investigations into the characteristics of the ridge waveguides have been carried out successfully under different fabrication parameters. According to the experimental results pre-

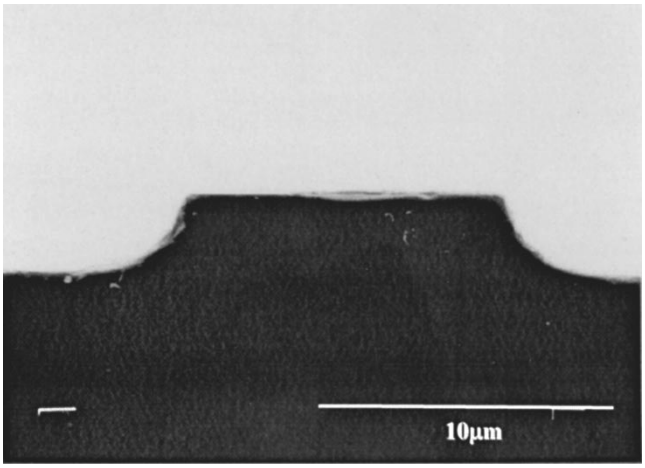

(a)

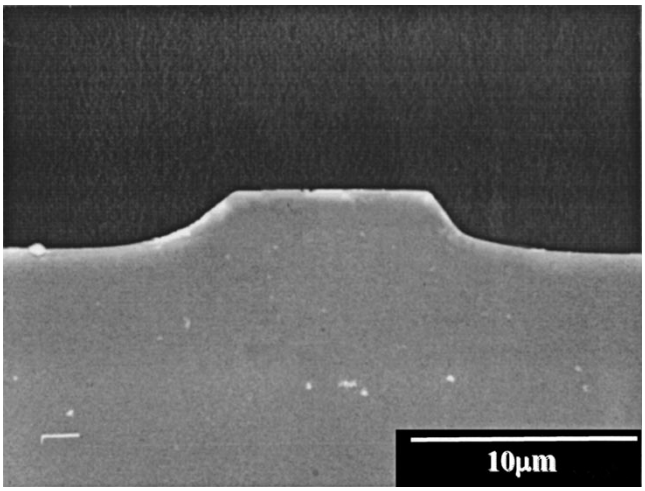

(b)

Fig. 10. Cross-sectional SEM photograph of the ridge waveguides: (a) the ED process and (b) the self-aligned process. For both cases: PE at 240 °C for 6 h and wet etching in HF for 6 h.

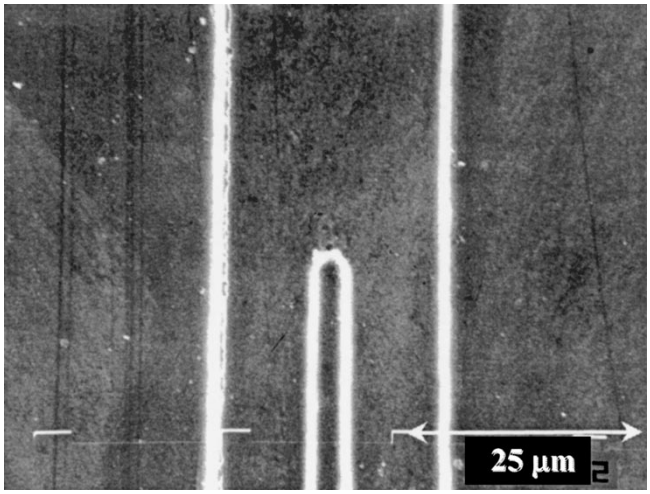

Fig. 11. SEM photograph from the top view at the Y-branch regions of a ridge waveguide Mach–Zehnder modulator in z-cut $LiNbO_3$.

sented, the NIPE effect influences the surface profile of the ridge waveguide, while the Ni-indiffusion induces the domain-inversion effect, which in turn influences the etch depth and surface roughness. Moreover, the self-aligned process was

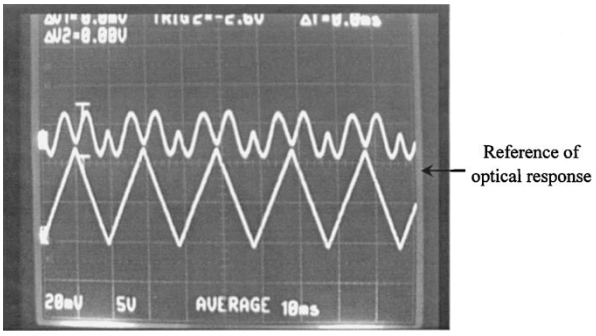

(a)

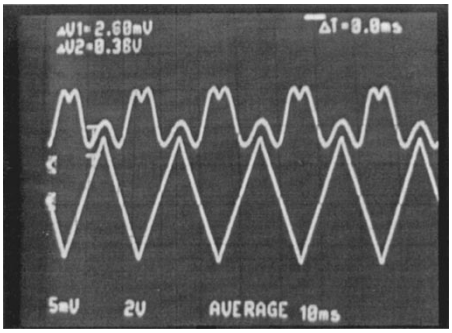

(b)

Fig. 12. Modulation output of the ridge waveguide Mach–Zehnder modulator fabricated by the self-aligned process: (a) at a wavelength of 0.6328 μm (lower trigger triangular-wave: 5 V/div, upper optical response: 20 mV/div) and (b) at a wavelength of 1.3 μm (lower trigger triangular-wave: 20 V/div, upper optical response: 5 mV/div).

successfully applied to the fabrication the ridge waveguide Mach–Zehnder modulator. The measured half-wave voltage is 20.5 V, and the extinction ratio is 12 dB at a wavelength of 1.3 μm. The measured half-wave voltage is 4.2 V, and the extinction ratio is 8 dB at a wavelength of 0.6328 μm. Owing to the use of the self-aligned technique, the proposed fabrication process has many advantages, such as the process simplification, yield improvement, suppression of unwanted planar waveguides, and high-coupling efficiency to a single-mode fiber, as compared to the conventional waveguide fabrication processes. Most importantly, this process requires only one photolithographic process. Hence, mask-aligned errors will be completely avoided by using the self-aligned Ni/Ti/Si structure. Thus, it is believed that the self-aligned fabrication process has a potential for further applications in the fabrication of integrated optics devices.

ACKNOWLEDGMENT

The authors would like to express their appreciation to Prof. W.-S. Wang and J. C. Smith for their encouragement and helpful suggestions.

REFERENCES

[1] K. Noguchi and K. Kawano, "Proposal for Ti : $LiNbO_3$ optical modulator with modulation bandwidth more than 150 GHz," *Electron. Lett.*, vol. 28, no. 18, pp. 1759–1761, 1992.

[2] G. K. Gopalakrishnan, C. H. Bulmer, W. K. Burns, R. W. McElhanon, and A. S. Greenblatt, "40 GHz, low half-wave voltage Ti:$LiNbO_3$ intensity modulator," *Electron. Lett.*, vol. 8, pp. 826–827, 1992.

[3] D. W. Dolfi and T. R. Ranganth, "50 GHz, velocity-matched broad wavelength $LiNbO_3$ modulator with multimode active section," *Electron. Lett.*, vol. 28, pp. 1197–1198, 1992.
[4] K. Kawano, T. Kitoh, H. Jumonji, T. Nozawa, and M. Yanagibashi, "New travelling-wave electrode Mach-Zehnder optical modulator with 20GHz bandwidth and 4.7 V driving voltage at 1.52 μm wavelength," *Electron. Lett.*, vol. 25, no. 20, pp. 1382–1383, 1989.
[5] K. Noguchi, K. Kawano, T. Nozawa, and T. Suzuki, "A $Ti:LiNbO_3$ optical intensity modulator with more than 20 GHz bandwidth and 5.2 V driving voltage," *IEEE Photon. Technol. Lett.*, vol. 3, pp. 333–335, 1991.
[6] K. Noguchi, O. Mitomi, K. Kawano, and M. Yanagibashi, "Highly-efficient 40-GHz bandwidth $Ti:LiNbO_3$ optical modulator employing ridge structure," *IEEE Photon. Technol. Lett.*, vol. 5, pp. 52–54, 1993.
[7] K. Noguchi, O. Mitomi, H. Miyazawa, and S. Seki, "A broadband $Ti:LiNbO_3$ optical modulator with a ridge structure," *J. Lightwave Technol.*, vol. 13, pp. 1164–1168, June 1995.
[8] C. L. Lee, and C. L. Lu, "CF_4 plasma etching on $LiNbO_3$," *Appl. Phys. Lett.*, vol. 35, pp. 756–758, 1979.
[9] J. L. Jackel, R. E. Howard, E. L. Hu, and S. P. Lyman, "Reactive ion etching of $LiNbO_3$," *Appl. Phys. Lett.*, vol. 38, pp. 907–909, 1981.
[10] F. Laurell, J. Webjorn, G. Arvidsson, and J. Holmberg, "Wet etching of proton-exchanged lithium niobateA novel processing technique," *J. Lightwave Technol.*, vol. 10, pp. 1606–1609, Nov. 1992.
[11] H. J. Lee and S. Y. Shin, "Lithium niobate ridge waveguides fabricated by wet etching," *Electron. Lett.*, vol. 31, no. 4, pp. 268–269, 1995.
[12] R. S. Cheng, W. L. Cheng, and W. S. Wang, "Mach-Zehnder modulators with lithium niobate ridge waveguides fabricated by proton-exchange wet etch and nickel indiffusion," *IEEE Photon. Technol. Lett.*, vol. 7, pp. 1282–1284, July 1995.
[13] R. S. Cheng, T. J. Wang, and W. S. Wang, "Wet-etched ridge waveguides in Y-cut lithium niobate," *J. Lightwave Technol.*, vol. 15, pp. 1880–1887, Oct. 1997.
[14] A. Campari, C. Ferrai, G. Mazzi, C. Summonte, S. M. Alshukri, A. Dewar, R. M. De La Rue, and A. C. G. Nutt, "Strain and surface damage induced by proton-exchange in Y-cut lithium niobate," *J. Appl. Phys.*, vol. 58, pp. 4521–4524, 1985.
[15] W. L. Chen, R. S. Cheng, J. H. Lee, and W. S. Wang, "Lithium niobate ridge waveguides by nickel diffusion and proton-exchanged wet-etching," *IEEE Photon. Technol. Lett.*, vol. 7, pp. 1318–1320, Nov. 1995.
[16] W. C. Chang, S. J. Chang, C. Y. Sue, and J. L. Shu, "Characteristics of proton-exchanged wet etching on Z-cut nickel-indiffused lithium niobate," *Microwave and Opt. Technol. Lett.*, July 1998.
[17] Y. P. Liao, D. J. Chen, R. C. Lu, and W. S. Wang, "Nickel-diffused lithium niobate optical waveguide with process-dependent polarization," *IEEE Photon. Technol. Lett.*, vol. 8, pp. 548–550, Apr. 1996.
[18] P. K. Wei and W. S. Wang, "Fabrication of lithium niobate optical channel waveguides by nickel indiffusion," *Microwave Opt. Technol. Lett.*, vol. 7, no. 5, pp. 219–221, 1994.

Wen-Ching Chang was born in Pingtung, Taiwan in 1963. He received the B.E. degree in electronic engineering from Tamkang University, Taipei, Taiwan, in 1985. He received the M.S. and Ph.D. degrees in electrical engineering from the National Taiwan University, Taipei, in 1987 and 1993, respectively.

From 1985 to 1993, he was engaged in research on the fabrication or simulation of optoelectronic devices, such as $LiNbO_3$ waveguide modulators, the beam propagation method, and nonlinear integrated optics. He joined the Department of Electrical Engineering at Tamkang University in 1993 as an Associate Professor. Meanwhile, he focused on the fabrication of the NIPE ridge waveguide in collaboration with the Integrated Optics Laboratory of the Department of Electrical Engineering at the National Taiwan University. His current research interests concentrate on the design of smart photonic logic gates including $LiNbO_3$ and semiconductor optoelectronic technologies and their applications on the WDM networks.

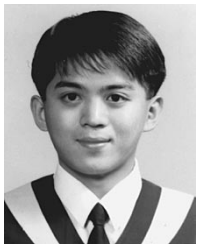

Chao-Yung Sue was born in Taipei, Taiwan, in 1973. He received the B.E. degree in electrical engineering from the National Cheng-Kung University, Tainan, Taiwan, in 1996. He received the M.E. degree in electrical engineering from Tamkang University, Taipei, in 1998.

His current research focuses on the design and fabrication of integrated optical devices.

Hung-Ching Hou was born in Kaohsiung, Taiwan, in 1973. He received the B.E. degree in electrical engineering from the Chinese Engineering College, Taiwan, in 1996. He received the M.E. degree in electrical engineering from Tamkang University, Taipei, Taiwan, in 1997.

His current research interests concentrate on the design and fabrication of integrated optical devices.

Shih-Jung Chang was born in Taiwan. He received the B.S. degree in physics and the M.E. degree in electrical engineering from the National Taiwan University, Taipei, Taiwan. He is currently pursuing the Ph.D. degree in electrical engineering at the same university.

His current research interests concentrate on the design and fabrication of integrated optical devices.

Pei-Kuen Wei was born in Taiwan. He received the B.S. degree in mechanical engineering and the Ph.D. degree (1995) in electrical engineering from the National Taiwan University, Taipei, Taiwan.

He joined the Institute of Atomic and Molecular Sciences, Academia Sinica, Taipei, in 1995. His current research interests concentrate on the theory, measurement, and characterization of optical fiber and guided-wave optical devices.